PROBING LUNAR POLAR IMPACT CRATERS USING FULL-POL L-BAND CHANDRAYAAN-2 DUAL-FREQUENCY SAR (DFSAR). Tathagata Chakraborty*, Sriram S. Bhiravarasu, Anup Das, Dharmendra Kr. Pandey, Deepak Putrevu, Arundhati Misra, Raj Kumar and the DFSAR Team, Space Applications Centre, Indian Space Research Organization, Ahmedabad, India *(tathagata@sac.isro.gov.in)

Introduction: The L&S band Dual-Frequency Synthetic Aperture Radar (DFSAR) onboard Chandrayaan-2 orbiter, is the first fully (quad) polarimetric SAR system in the lunar orbit **[1]**. The architecture of this radar instrument supports multiple polarimetric modes of operation. DFSAR observations contribute significantly towards understanding the origin and evolution of lunar impact craters **[2]**. In the present study, we exhibit some initial results obtained from DFSAR L-band Full-Polarimetric (FP) observations towards understanding physical behaviour of two different groups of impact craters.

Study Area and Data Used: L-band FP SAR observations obtained at 26º incidence angle over secondary craters situated on the floor of Peary Crater (87.9ºN, 35.3ºE) in the lunar north polar region are analysed. This region consists of one young, fresh crater and two craters that were classified as CPR anomalous craters in previous studies **[3]** (Fig. 1). For comparison, CPR product derived from S-band zoom mode SAR data of the same region acquired by LRO Mini-RF are used.

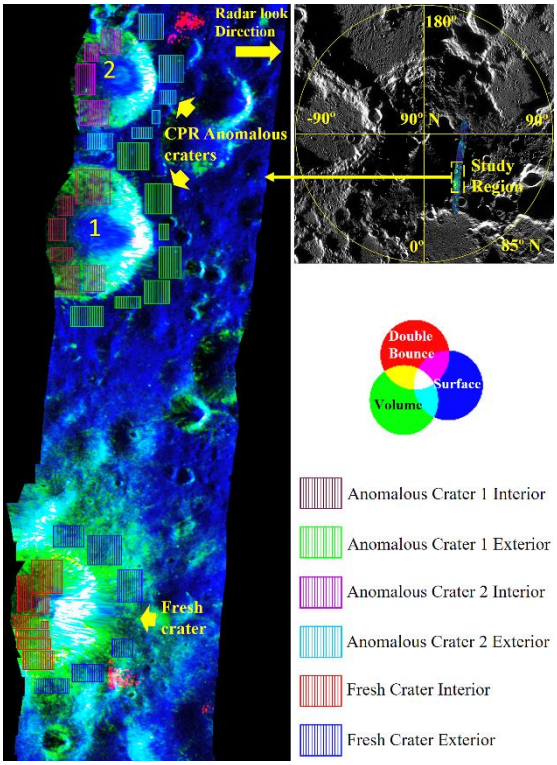

Figure 1: RGB composite of double bounce (red), volume (green) and surface (blue) radar scattering component derived from Yamaguchi four-component (Y4R) decomposition method. The location of the craters are shown in inset overlaid on LROC-WAC mosaic of lunar north pole.

Method: The methodology followed to analyse DFSAR data using ESA PolSARPro is described below:

i. Covariance and Coherency Matrix: The complex co-polarized (HH and VV) and cross-polarized (HV and VH) backscattering elements are used to generate covariance matrix (C_3) and coherency matrix (T_3) assuming symmetry between cross-polarized channels (HV and VH) **[4]**. The derived C_3 and T_3 parameters are multilooked (with a factor of 38) to generate squared pixels with reduced speckle noise.

ii. Circular Polarization Ratio (CPR): The C_3 matrix is converted to a C_2 matrix corresponding to Compact-Pol (CP) scattering elements **[5]** considering left circular transmission and linear reception geometry. The resultant complex CP (LH and LV) backscattering elements are used for computation of Stokes parameters and CPR **[6]**.

iii. Polarimetric Entropy and Alpha: The three eigenvalues of the T_3 matrix is utilized to derive two major polarimetric parameters named Entropy (H) and the Mean Alpha angle ($\bar{\alpha}$) **[4]**. The Entropy value indicates the degree of randomness in the scatterer and depolarization of the microwave energy. If entropy is low (H<0.3), then the scatterers are coherent and strongly polarized **[7]**. In contrary, high entropy can be produced by distributed (incoherent) targets resulting in highly depolarized scattering. The mean scattering angle alpha ($\bar{\alpha}$) is useful to understand the nature of scatterer along with the type of scattering triggered by the target. The mean alpha angle, $\bar{\alpha}$, value varies from 0° to 90°. $\bar{\alpha} \leq 40°$ represents surface scattering, $\bar{\alpha} \geq 40°$ but less than 60° represents volume scattering and very high $\bar{\alpha}$ value (i.e. $\geq$ 60°) represents double bounce scattering from the target **[4]**. Thus, for lunar surface, low values of $\bar{\alpha}$ (~25°) correspond to smooth regolith surface, moderate $\bar{\alpha}$ values (~45°) represent wavelength scale roughness and ejecta distribution and very high $\bar{\alpha}$ ($\geq$ 60°) may be characteristic of dihedral joints /debris boulder distribution.

iv. Full-Pol Decomposition: In order to characterize the lunar impact craters and ejecta distributions, the Yamaguchi four-component (Y4R) scattering power decomposition method with orientation angle correction **[8]**, **[9]** is used in the study. This method is applicable to a heterogeneous surface with significant roughness and distributed targets. According to this decomposition theorem, from the coherency matrix four received powers corresponding to surface, double bounce, volume and helix-scattering are determined.

v. Ground Projection and Ortho-rectification: The polarimetric products are georeferenced and orthorectified using a LOLA DEM (30 m/pix) **[10]**. The georeferenced products have a resolution of 25 m/pixel.

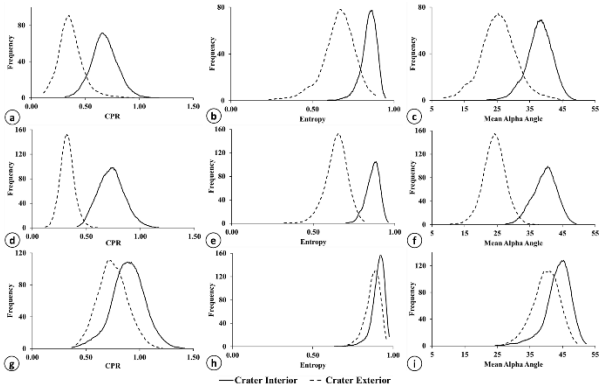

Figure 2: The distribution of CPR, Entropy and Mean Alpha angle in the interior and exterior part of the CPR Anomalous crater 2 (***a, b, c***), CPR Anomalous crater 1 (***d, e, f***) and Fresh crater (***g, h, i***) respectively.

Results: Here, we investigate the CPR, Entropy and mean Alpha value of the interior and exterior part of the two anomalous craters and a fresh crater. The average values of CPR, Entropy and mean Alpha corresponding to the fresh crater are higher than those of anomalous craters (Fig. 2). The distribution of mean CPR, entropy and alpha angle at the interior and exterior of the fresh crater are almost identical, indicating that the roughness of the two areas are, on an average, the same on the scale of centimeters to decimeters. Higher values of mean entropy (~0.87) and alpha angle (~41°) clearly indicate the presence of a dominant volume scattering component at regions both inside and outside of the fresh crater. The difference between values in the interior and exterior part of the anomalous craters much higher compared to the fresh crater. Due to smoother surface, the CPR, Entropy and mean Alpha values in the exterior part of the anomalous craters are comparatively much lesser than interior part. However, reason behind the enhancement in these parameters in the interior part of the anomalous craters is still under investigation. None of the craters show significant double bounce scattering. Hence, prevalence of several meter scale ejecta blocks is minimal, even in fresh crater.

Mini-RF observations also reveal similar results and is in good agreement with the DFSAR observations (Fig. 3). However, due to shorter wavelength (S-band) the Mini-RF CPR values are comparatively higher than DFSAR observations. Fig. 3 reveals an interesting observation – while the mean CPR values for fresh crater interior and ejecta are identical at L- and S-band, they are different for anomalous craters, analysed in this study. For the anomalous crater regions, the S-band CPR is higher in the exterior region compared to that in L-band, implying differences in the material properties and roughness present. For the fresh crater region, similar CPR values at both L- and S-band indicate the presence of volumetric scatterers or roughness at cm and larger scales. In the case of anomalous crater, the roughness responsible for S-band enhancement do not cause a similar enhancement in L-band, indicating that they are too small to be resolved by the longer-wavelength (L-band) signals.

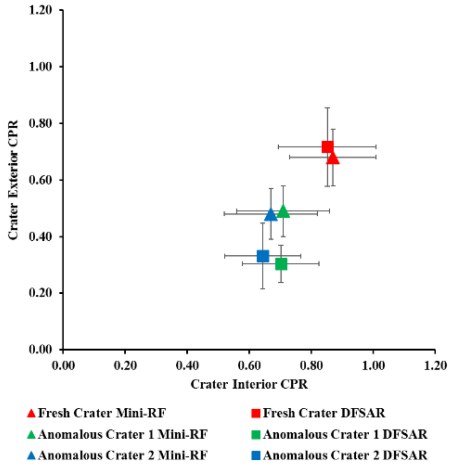

Figure 3: Average CPR values in the interior and exterior parts of various craters imaged by LRO Mini-RF (S-band) CP data and CH2 DFSAR (L-band) FP data. The ***triangular data points*** correspond to Mini-RF data and ***square data points*** correspond to DFSAR data

It is evident that, both interior and exterior part of the fresh crater shows equivalent volume and surface scattering due to similar ejecta and roughness distribution in both parts of the crater (Fig.1). However, volume scattering plays dominant role from the interior part of the anomalous craters. In contrast, volume scattering component in the exterior part of the anomalous craters drastically reduces leading to dominance of surface scattering in the region. Hence, the surface scattering component is the background scattering from the lunar average smooth surface, and the volume scattering component majorly depicting the variability in the wavelength scale roughness associated with lunar ejecta. As the sampled craters are devoid of several meter scale ejecta or debris blocks, hence, minimal occurrence of double bounce is observed. Although, with increase in the meter scale ejecta blocks, enhancement in the double bounce, CPR and mean alpha angle value is expected. Thus, by exploiting polarimetric parameters derived from full-pol data, new insights into the physical behaviour of the lunar surface can be attained.

References: [1] Putrevu, D. et al. (2016) *Adv. Space Res.*, 57, 627-646. [2] Putrevu, D. et al., (2020), 51st LPSC, Abstract#1420. [3] Spudis, P.D. et al. (2013), *JGR*, 118, 2016–2029. [4] Cloude, S.R., and Pottier, E. (1997) IEEE TGRS, 35(1), 68-78. [5] Raney, R.K. (2016) *IEEE GRSL*, 13 (6), 861-864. [6] Raney, R.K. et al. (2012) *JGR*, 117, E00H21. [7] Singh, G. et al. (2013) *IEEE TGRS*, 52(2), 1177-1196. [8] Lee, J.S., and Ainsworth, T.L. (2010) *IEEE TGRS*, 49(1), 53-64. [9] Yamaguchi, Y. et al. (2010) *IEEE TGRS*, 49(6), 2251-2258. [10] Mazarico, E. et al. (2011), *Icarus*, 211, 1066–1081